Dual synchronization of chaos in one-way coupled microchip lasers

A. Uchida, S. Kinugawa, T. Matsuura, and S. Yoshimori
Department of Electronics and Computer Systems, Takushoku University, 815-1 Tatemachi, Hachioji, Tokyo 193-0985, Japan
(Received 29 July 2002; published 27 February 2003)

We experimentally demonstrate the dual synchronization of chaos in two pairs of Nd:YVO_4 microchip lasers in a one-way coupling configuration over one transmission channel. Dual synchronization is achieved when the optical frequency is matched between the corresponding pairs of lasers by using injection locking. We investigate the influence of optical injection from the two master lasers to one slave laser, and found that the dual synchronization is observed when the injection locking is achieved between either of the master lasers and the slave laser. Under the condition of the injection locking between both of the master lasers and the slave laser, the injection locking is alternately achieved and the accuracy of dual synchronization is degraded. We also confirm these results by numerical calculation.

DOI: 10.1103/PhysRevE.67.026220 PACS number(s): 05.45.Xt, 42.65.Sf, 42.55.Rz

I. INTRODUCTION

The technique of synchronization of chaos in laser systems has a potential for applications of optical secure communications and spread spectrum communications [1,2]. Synchronization of chaos is used to share the same chaos in the transmitter and the receiver as a cryptographical code. Many studies on the synchronization of chaos have been reported in one-way coupled laser systems so far for the purpose of optical communications. However, since the configuration of synchronization is limited to a single pair of lasers, this method cannot be applied for multiuser communication systems [3]. From the dynamic point of view, synchronization of chaos in multiple pairs of lasers is a very interesting topic.

There have been many studies on the synchronization of chaos in multiple lasers or laser arrays [4–6]. In these configurations, the laser beams are mutually coupled to each other, and the chaotic dynamics of coupled lasers are totally different from those of a solitary laser. This configuration is not used for optical communications, in which a chaotic wave form in the transmitter must not be changed after transmission to the receiver. Thus we need to employ a synchronization technique of chaos in one-way coupled lasers with multiple pairs.

Multiplexing chaos using synchronization has been reported in a simple map and electronic circuit model by Tsimring and Sushchik [7]. Dual synchronization of chaos has also been investigated to synchronize two different pairs of chaotic maps and delay-differential equations by Liu and Davis [8]. To synchronize each pair of chaotic systems, all the parameter settings must be identical between the transmitter and the receiver, whereas they must be slightly shifted between different pairs of chaotic systems. Although it has been shown theoretically in Refs. [7,8] that it is possible to synchronize each pair of multiplexed chaotic oscillators, these multiplexing synchronization methods have not been directly applied to chaos in laser experiments. In particular, the injection-locking effect has not been investigated to achieve dual synchronization in these studies, although the injection-locking effect is very important for synchronization of chaos in laser systems [9]. It is necessary to investigate synchronization of multiplexing chaos in laser systems for multiuser optical communications using chaos.

In this paper, we experimentally demonstrate the dual synchronization of chaos in two pairs of Nd:YVO_4 microchip lasers in a one-way coupling configuration over one-transmission channel. We changed the optical frequency of each laser and controlled the condition of injection locking to achieve dual synchronization between the corresponding pairs in the transmitter and the receiver, instead of the matching of internal parameters, which has been done in the previous studies of Refs. [7,8]. We also investigate the characteristics of dual synchronization by both experiment and numerical simulations when the injection-locking condition is changed.

II. EXPERIMENT

A. Setup

Figure 1 shows our experimental setup for the dual synchronization of chaos. We use four Nd:YVO_4 microchip crystals (1.1 at. % doped; II-VI Inc.), which were obtained from the same crystal rod. Each crystal is pumped by an individual laser diode (Coherent Inc., DCF81-1000C-100-FC) with two focusing lenses. We set each microchip laser to oscillate with a single-longitudinal mode at a low pumping power. The temperatures of the microchip crystals and the laser diodes are controlled by thermoelectric coolers (resolution of 0.01 K) for fine tuning of the laser frequencies. Two of the microchip lasers are used as master lasers, which we will refer to as "$M1$" for master laser 1 and "$M2$" for master laser 2. The other two lasers are used as slave lasers ("$S1$" for slave laser 1 and "$S2$" for slave laser 2). For $M1$ and $M2$, the injection current of a laser diode used for pumping is sinusoidally modulated to obtain chaotic pulsation. A fraction of the master laser outputs is mixed at a beam splitter and propagates through one-transmission channel in a free space (the thick solid lines in Fig. 1). The combined signals of $M1$ and $M2$ are injected into the two slave laser cavities for dual synchronization. An optical isolator for each master laser is used to achieve one-way coupling with an isolation of -60 dB. Chaotic temporal wave forms of the four lasers are simultaneously detected with photodiodes and

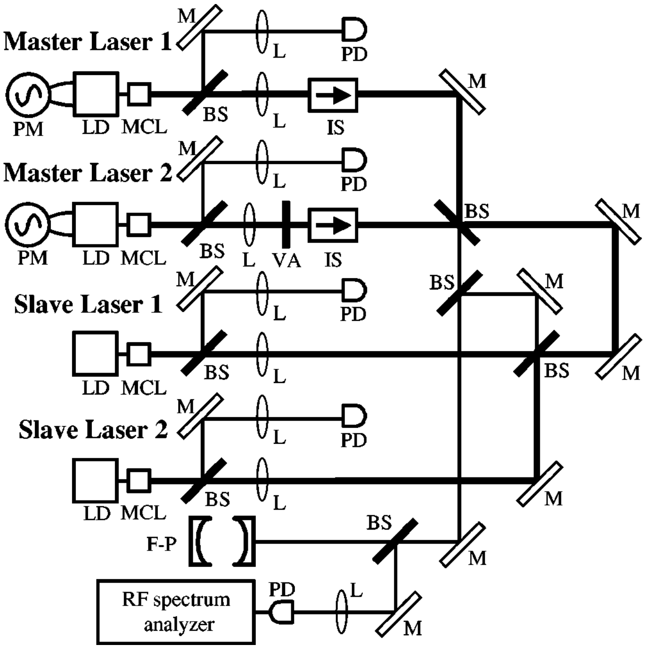

FIG. 1. Experimental setup for dual synchronization of chaos. BS, beam splitter; F-P, Fabry-Perot interferometer; IS, optical isolator; L, lense; LD laser diode; M, mirror; MCL, Nd:YVO_4 microchip laser; PD, photodiode; PM, pump modulation; VA, variable attenuator.

a digital oscilloscope (Sony Tektronix, TDS420). The optical spectra of the lasers are measured with a Fabry-Perot scanning interferometer (TEC-Optics, SA-7.5). The beat frequencies between the four lasers are measured with a radio-frequency (rf) spectrum analyzer (Advantest, R3131) through a photodiode.

The modulation frequencies of the pumping laser diodes are 2.46 MHz and 2.43 MHz for the master and slave lasers, and the relaxation oscillation frequencies of the master and slaver lasers are 0.700 MHz and 0.640 MHz, respectively. Note that the fundamental oscillation frequencies of chaotic wave forms are dependent upon the relaxation oscillation frequencies rather than the modulation frequencies. The other laser parameters used in our experiments are as follows: the injection currents of the laser diodes are $J_{M1} = 243$ mA, $J_{M2} = 342$ mA, $J_{S1} = 339$ mA, and $J_{S2} = 332$ mA, where the subscripts indicate the corresponding laser. The temperatures of the laser diodes for pumping are set to 298.00 K for all laser diodes. The temperatures of the microchip lasers are $T_{M1} = 295.18$ K, $T_{M2} = 300.50$ K, $T_{S1} = 298.00$ K, and $T_{S2} = 298.00$ K. The injection powers of the master lasers are set to $P_{M1,S1} = 0.139$ mW and $P_{M2,S1} = 0.095$ mW measured in front of $S1$, and $P_{M1,S2} = 0.193$ mW, $P_{M2,S2} = 0.133$ mW measured in front of $S2$. The powers of the slave lasers are $P_{S1} = 2.81$ mW and $P_{S2} = 2.87$ mW, respectively.

B. Experimental results

Injection locking is a very important phenomenon for chaos synchronization [9,10]. The optical frequencies of our microchip lasers are tuned linearly as functions of the temperature of the crystals at 1.2 GHz/K. First we adjust the temperatures of $M1$ and $M2$ to obtain injection-locking between the optical frequencies of a pair of $M1$ and $S1$ (refered to as "$M1$-$S1$"), and a pair of "$M2$-$S2$" by monitoring the spectra on the Fabry-Perot scanning interferometer. Then we observe six peaks of frequency beats between the four lasers on the rf spectrum analyzer. When two of the beat frequencies for $M1$-$S1$ and $M2$-$S2$ are adjusted within the injection-locking ranges (100 and 80 MHz, respectively) with more accurate temperature control of $M1$ and $M2$, the two beat frequencies disappear and the two laser frequencies in each pair for $M1$-$S1$ and $M2$-$S2$ are perfectly matched. Conversely, the other beat frequencies for $M1$-$S2$, $M2$-$S1$, $M1$-$M2$, and $S1$-$S2$ remain at the same frequency of 1.6 GHz, which is out of the injection-locking range. In this case, the injection-locking effect is achieved only for $M1$-$S1$ and $M2$-$S2$, not for the other coupling combinations.

Figure 2 shows the temporal wave forms and their correlation plots of $M1$-$S1$ [Figs. 2(a) and 2(b)], $M2$-$S2$ [Figs. 2(c) and 2(d)], $M1$-$S2$ [Figs. 2(e) and 2(f)], and $M2$-$S1$ [Figs. 2(g) and 2(h)]. Synchronization of chaos is achieved between the corresponding pairs of $M1$-$S1$ and $M2$-$S2$ independently under injection-locking, whereas it is not achieved for $M1$-$S2$ and $M2$-$S1$. The $S1$ laser reproduces the $M1$ component separately from the injection signal of the combination of $M1$ and $M2$. The output of $S2$ is also synchronized with only the $M2$ component although the combined signal of $M1$ and $M2$ is injected. Thus, we have achieved dual synchronization of chaos in two pairs of microchip lasers.

It can be seen in Fig. 2 that the injection signal from $M2$ to $S1$ has no influence on the synchronization between $M1$ and $S1$. To investigate the influence of the $M2$ signal on the synchronization of $M1$-$S1$, we change the beat frequency of $M2$-$S1$ maintaining the synchronization of $M1$-$S1$ and $M2$-$S2$ under their injection-locking conditions of 100 and 80 MHz, respectively. We change the temperatures of $M2$ and $S2$ simultaneously to maintain synchronization of $M2$-$S2$. As the beat frequency of $M2$-$S1$ is decreased from 1.6 GHz to 0 MHz, the synchronization of chaos between $M1$ and $S1$ degrades due to the interference of $M2$ on $S1$. Here, we quantitatively estimate the accuracy of synchronization as variance of the normalized correlation plot from a best-fit linear relation [9] as follows:

$$\sigma^2 = \frac{1}{N} \sum_{i}^{N} (I_{\mathrm{m,i}} - I_{\mathrm{s,i}})^2, \tag{2.1}$$

where N is the total number of samplings of the temporal wave forms (15 000 points), $I_{m,i}$ and $I_{s,i}$ are the normalized intensities of the master and slave lasers at the ith sampling point. A smaller variance σ^2 implies higher accuracy of chaos synchronization. We measure the accuracy for $M1$-$S1$ as a function of the beat frequency of $M2$-$S1$ at three different injection powers of $M2$, as shown in Fig. 3(a). At a large injection power [the thick solid curve in Fig. 3(a)], the accuracy degrades as the beat frequency is decreased, because the injection-locking effect between $M2$ and $S1$ improves. At a

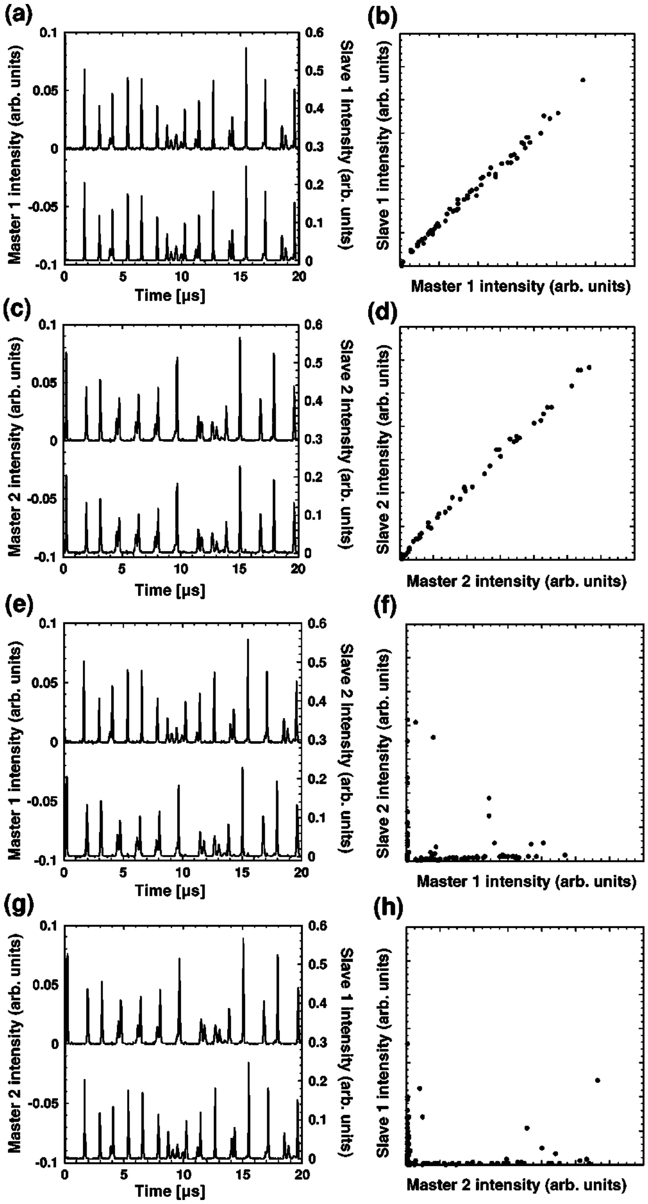

FIG. 2. Temporal wave forms and their correlation plots for the pair of $M1$-$S1$ [(a), (b)], $M2$-$S2$ [(c), (d)], $M1$-$S2$ [(e), (f)], and $M2$-$S1$ [(g), (h)].

small injection power (the thin solid curve), synchronization does not degrade due to less influence from the $M2$ injection. We also continuously change the injection power of $M2$ by varying the transmittance of the variable attenuator for $M2$ while the beat frequency of $M2$-$S1$ is fixed, as shown in Fig. 3(b). As the injection power is increased, a degeneration of synchronization is observed at a small beat frequency of $M2$-$S1$ [the thick solid curve in Fig. 3(b)] due to the strong injection of the $M2$ signal. Therefore, when we satisfy the conditions to achieve injection locking between $M2$ and $S1$, less synchronization of chaos is observed between $M1$ and $S1$.

The condition for achieving dual synchronization is dependent upon an injection-locking range that is different from the case of a single pair of microchip lasers [9]. The frequency dynamics of an injection-locked laser with two different injection lights are very important for the achievement of dual synchronization. We therefore investigate the accuracy of dual synchronization when the optical frequency of $M2$ approaches the optical frequencies of $M1$ and $S1$, which are locked all the time. Figure 4 shows the corresponding correlation plots of $M1$-$S1$ and $M2$-$S1$ at the beat frequencies of $M2$-$M1$ of 1 GHz and 100 MHz. Synchronization of chaos is achieved between $M1$-$S1$ [Fig. 4(a)], and no linear correlation appears in the correlation plots of $M2$-$S1$ [Fig. 4(b)], since the frequency of $M2$ is far from the frequencies of $M1$ and $S1$. Conversely, as the beat frequency of $M2$-$M1$ is decreased to 100 MHz, the correlation of $M1$-$S1$ is degraded and that of $M2$-$S1$ is improved as shown in Figs. 4(c) and 4(d). The accuracy of synchronization for $M2$-$S1$ is better than that for $M1$-$S1$ at the small beat frequency of 100 MHz. In this case, a part of the $S1$ component is pulled to the frequency of $M2$, and there is a partial injection-locking between $M2$ and $S1$. Therefore, the frequency pulling effect between $M2$ and $S1$ reduces the accuracy of synchronization of $M1$-$S1$.

We investigate the change of accuracy systematically as the frequency of $M2$ is changed. Figure 5 shows the accuracy of synchronization for $M1$-$S1$ (the solid curve) and $M2$-$S1$ (the dotted curve) as a function of the detuning of $M2$-$M1$. The accuracy of synchronization is varied between $M1$-$S1$ and $M2$-$S1$ as the detuning of $M2$-$M1$ is changed. When the frequency of $M2$ approaches the initial value of the frequency of $S1$ (where the detuning of $M1$-$M2$ is -150 MHz), the most accurate value for $M2$-$S1$ and the least accurate value for $M1$-$S1$ are observed. These curves indicate that the accuracy of synchronization for $M2$-$S1$ is improved as the frequency pulling effect between $M2$ and $S1$ is gradually increased.

III. NUMERICAL CALCULATION

A. Model

To confirm our experimental observations, we numerically calculate a model for dual synchronization using microchip lasers. We expand the Tang-Statz-deMars equations [9,11] for the dual synchronization of four microchip lasers. The rate equations are described as follows:

Master 1

$$\frac{dn_{0,m1}}{dt}=w_{0,m1}[1+w_{\mathrm{p},m1}\cos(2\pi\tau f_{\mathrm{p},m1}t+\Phi_{m1})]-n_{0,m1} -\left(n_{0,m1}-\frac{n_{1,m1}}{2}\right)E_{m1}^2, \tag{3.1}$$

$$\frac{dn_{1,m1}}{dt}=-n_{1,m1}+(n_{0,m1}-n_{1,m1})E_{m1}^2, \tag{3.2}$$

$$\frac{dE_{m1}}{dt}=\frac{K_{m1}}{2}\left[\left(n_{0,\mathrm{m1}}-\frac{\mathrm{n}_{1,\mathrm{m1}}}{2}\right)-1\right]E_{m1}; \tag{3.3}$$

Master 2

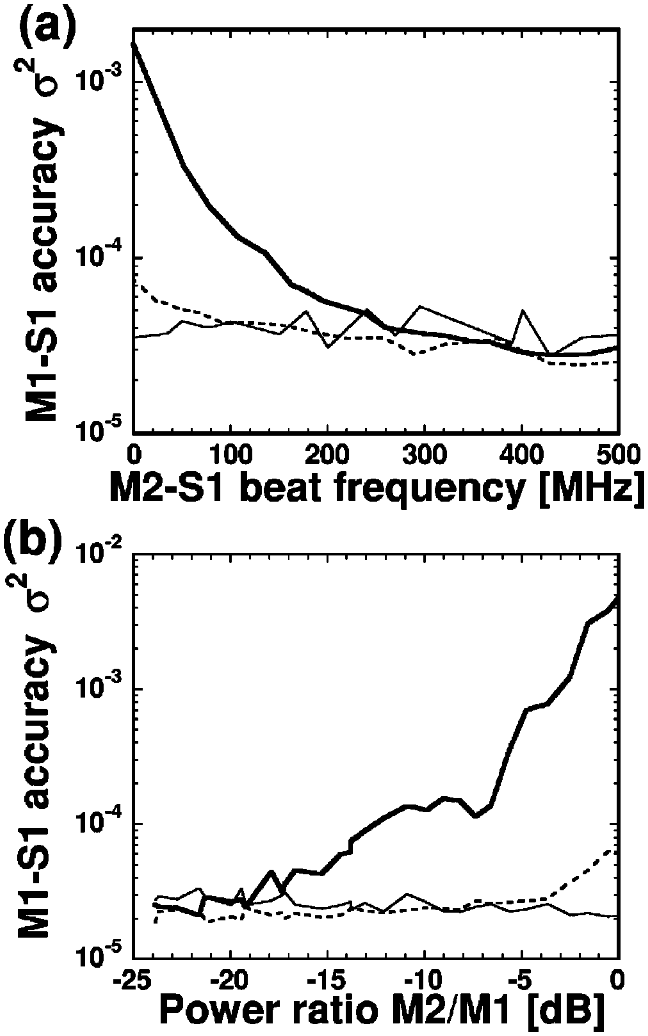

FIG. 3. Accuracy of chaos synchronization for the pair of $M1$-$S1$ as functions of (a) the beat frequency of $M2$-$S1$, and (b) the injection power ratio of $M2$ to $M1$. (a) The power ratio was fixed at -2.5 dB for the thick solid curve, -14 dB for the dotted curve, and -21 dB for the thin solid curve. (b) The beat frequency is fixed at 50 MHz for the thick solid curve, 260 MHz for the dotted curve, and 500 MHz for the thin solid curve.

$$\frac{dn_{0,m2}}{dt}=w_{0,m2}[1+w_{\mathrm{p},m2}\cos(2\pi\tau f_{\mathrm{p},m2}t+\Phi_{m2})]-n_{0,m2}-\left(n_{0,m2}-\frac{n_{1,m2}}{2}\right)E_{m2}^2, \tag{3.4}$$

$$\frac{dn_{1,m2}}{dt}=-n_{1,m2}+(n_{0,m2}-n_{1,m2})E_{m2}^2, \tag{3.5}$$

$$\frac{dE_{m2}}{dt}=\frac{K_{m2}}{2}\left[\left(n_{0,m2}-\frac{n_{1,m2}}{2}\right)-1\right]E_{m2}; \tag{3.6}$$

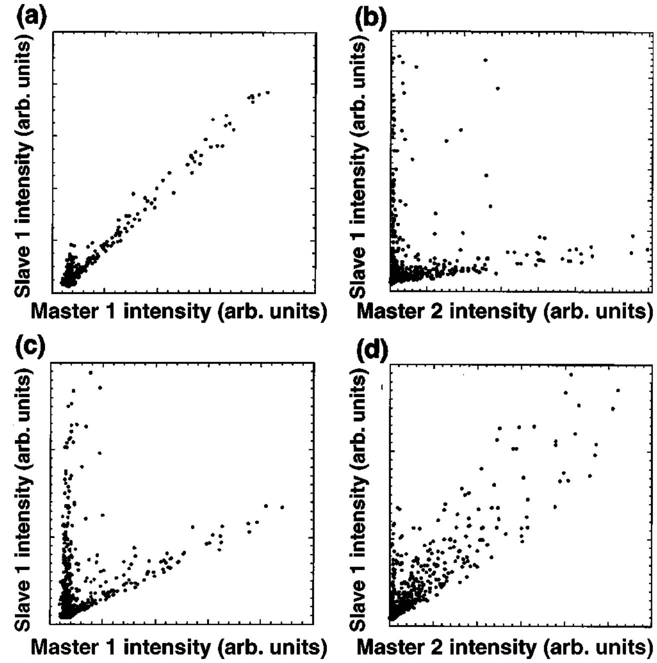

FIG. 4. Correlation plots for $M1$-$S1$ [(a), (c)] and $M2$-$S1$ [(b), (d)]. (a),(b) The beat frequency of $M2$-$M1$ is 1 GHz. (c),(d) The beat frequency of $M2$-$M1$ is 100 MHz.

Slave 1

$$\frac{dn_{0,s1}}{dt}=w_{0,s1}-n_{0,s1}-\left(n_{0,s1}-\frac{n_{1,s1}}{2}\right)E_{s1}^2, \tag{3.7}$$

$$\frac{dn_{1,s1}}{dt}=-n_{1,s1}+(n_{0,s1}-n_{1,s1})E_{s1}^2, \tag{3.8}$$

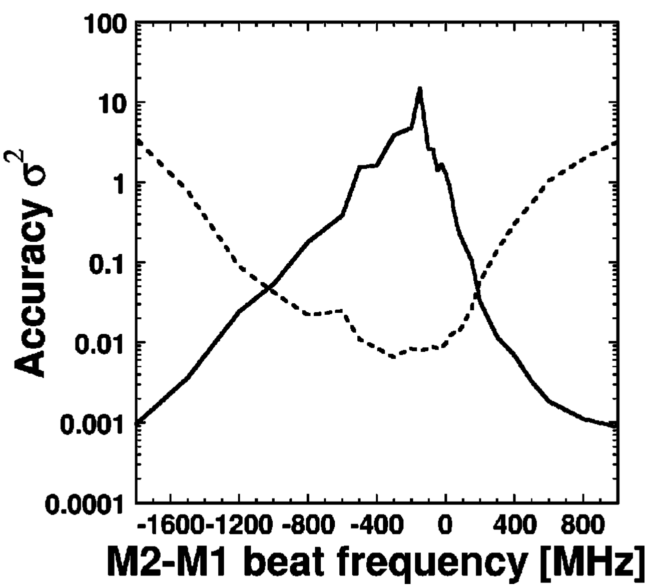

FIG. 5. Accuracy of chaos synchronization for the pair of $M1$-$S1$ (the solid curve) and $M2$-$S1$ (the dotted curve) as a function of the beat frequency of $M2$-$M1$.

$$\frac{dE_{s1}}{dt}=\frac{K_{s1}}{2}\left[\left(n_{0,s1}-\frac{n_{1,s1}}{2}\right)-1\right]E_{s1}+\frac{K_{s1}}{2}\beta_{11}E_{m1}\cos(\Delta\mu_{m1,s1})+\frac{K_{s1}}{2}\beta_{21}E_{m2}\cos(\Delta\mu_{m2,s1}); \tag{3.9}$$

Slave 2

$$\frac{dn_{0,s2}}{dt}=w_{0,s2}-n_{0,s2}-\left(n_{0,s2}-\frac{n_{1,s2}}{2}\right)E_{s2}^2, \tag{3.10}$$

$$\frac{dn_{1,s2}}{dt}=-n_{1,s2}+(n_{0,s2}-n_{1,s2})E_{s2}^2, \tag{3.11}$$

$$\frac{dE_{s2}}{dt}=\frac{K_{s2}}{2}\left[\left(n_{0,s2}-\frac{n_{1,s2}}{2}\right)-1\right]E_{s2}+\frac{K_{s2}}{2}\beta_{12}E_{m1}\cos(\Delta\mu_{m1,s2})+\frac{K_{s2}}{2}\beta_{22}E_{m2}\cos(\Delta\mu_{m2,s2}); \tag{3.12}$$

Phase difference

$$\frac{d(\Delta\mu_{m1,s1})}{dt}=2\pi\tau\Delta\nu_{m1,s1}-\frac{K_{s1}}{2}\beta_{11}\frac{E_{m1}}{E_{s1}}\sin(\Delta\mu_{m1,s1})-\frac{K_{s1}}{2}\beta_{21}\frac{E_{m2}}{E_{s1}}\sin(\Delta\mu_{m2,s1}), \tag{3.13}$$

$$\frac{d(\Delta\mu_{m2,s1})}{dt}=2\pi\tau\Delta\nu_{m2,s1}-\frac{K_{s1}}{2}\beta_{11}\frac{E_{m1}}{E_{s1}}\sin(\Delta\mu_{m1,s1})-\frac{K_{s1}}{2}\beta_{21}\frac{E_{m2}}{E_{s1}}\sin(\Delta\mu_{m2,s1}), \tag{3.14}$$

$$\frac{d(\Delta\mu_{m1,s2})}{dt}=2\pi\tau\Delta\nu_{m1,s2}-\frac{K_{s2}}{2}\beta_{12}\frac{E_{m1}}{E_{s2}}\sin(\Delta\mu_{m1,s2})-\frac{K_{s2}}{2}\beta_{22}\frac{E_{m2}}{E_{s2}}\sin(\Delta\mu_{m2,s2}), \tag{3.15}$$

$$\frac{d(\Delta\mu_{m2,s2})}{dt}=2\pi\tau\Delta\nu_{m2,s2}-\frac{K_{s2}}{2}\beta_{12}\frac{E_{m1}}{E_{s2}}\sin(\Delta\mu_{m1,s2})-\frac{K_{s2}}{2}\beta_{22}\frac{E_{m2}}{E_{s2}}\sin(\Delta\mu_{m2,s2}), \tag{3.16}$$

where n_0 and n_1 are the space-averaged and the first Fourier components, respectively, of population inversion density with spatial hole burning normalized by the threshold value. E is the normalized amplitude of the lasing electrical field. The subscripts $m1$, $m2$, $s1$, $s2$ indicate the master 1, master 2, slave 1, and slave 2 lasers, respectively. $\Delta\mu_{mi,sj}=\mu_{mi}-\mu_{sj}+2\pi\Delta\nu_{mi,sj}t$ is the phase difference of lasing field between the ith master and the jth slave lasers (i,j are 1 or 2). $\Delta\nu_{mi,sj}=\nu_{mi}-\nu_{sj}$ is the lasing frequency detuning between the ith master and the jth slave lasers. w_0 is the optical pump parameter scaled to the laser threshold. $K=\tau/\tau_p$, where τ is the upper state lifetime and τ_p is the photon lifetime in the laser cavity. β_{ij} is the coupling strength from the ith master to the jth slave lasers. w_p and f_p are the pump modulation amplitude and frequency. Φ is the initial phase of pump modulation. Time is scaled by τ. We use the fourth-order Runge-Kutta-Gill method to calculate these equations.

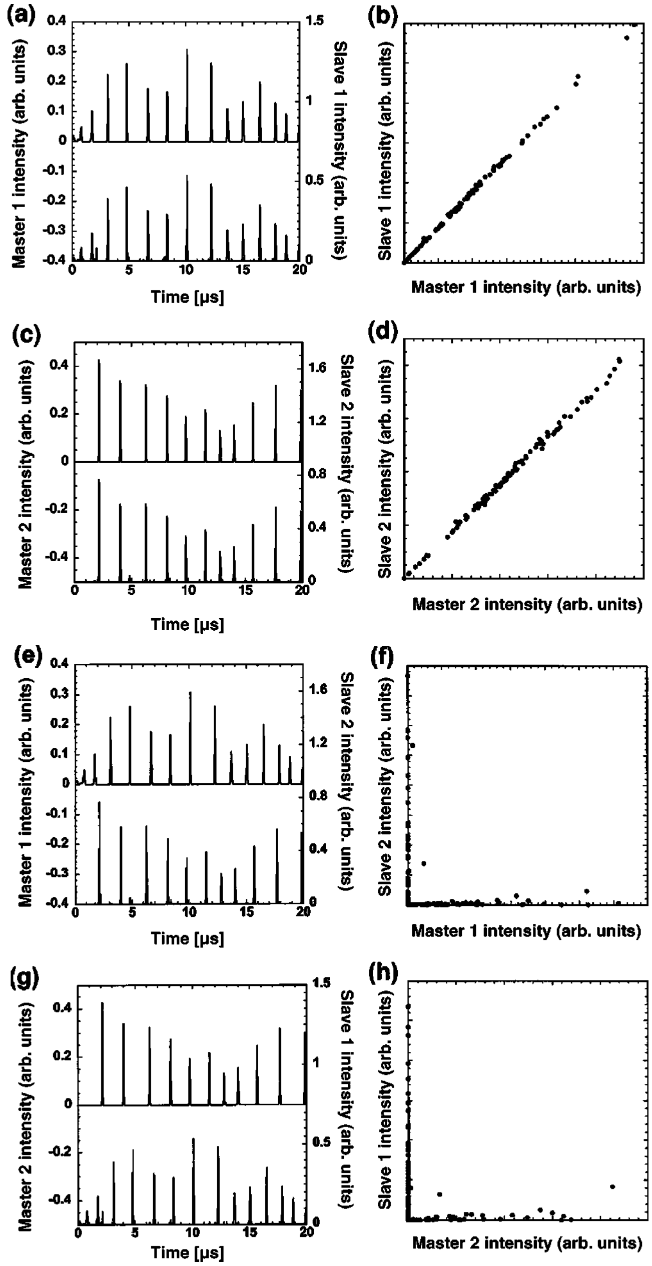

FIG. 6. Numerical results showing temporal wave forms and their correlation plots for the pair of $M1$-$S1$ [(a), (b)], $M2$-$S2$ [(c), (d)], $M1$-$S2$ [(e), (f)], and $M2$-$S1$ [(g), (h)].

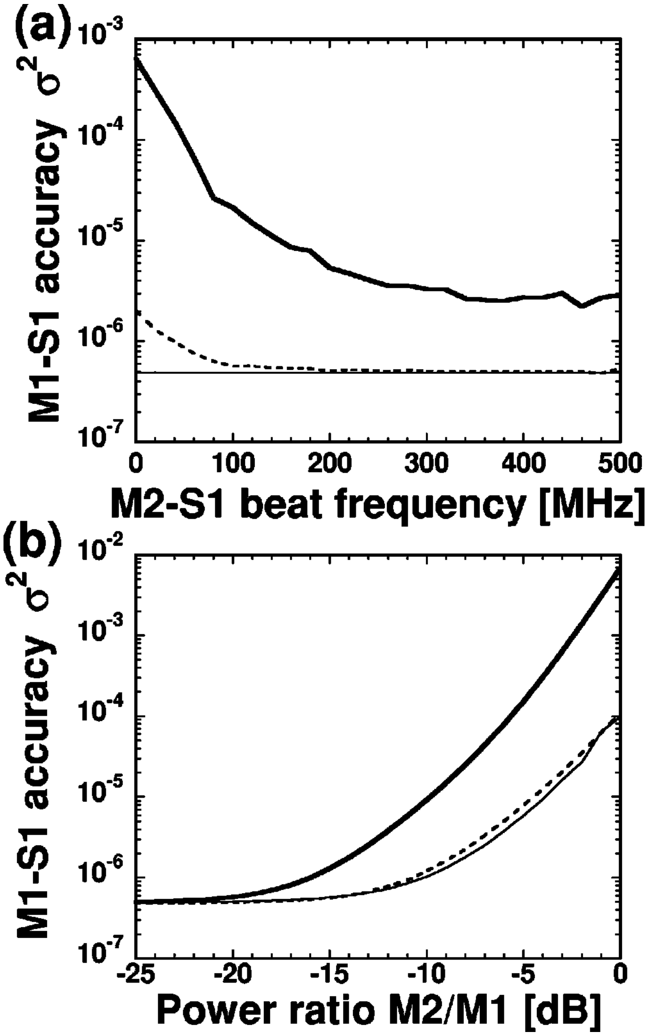

FIG. 7. Numerical results showing accuracy of chaos synchronization for the pair of $M1$-$S1$ as functions of (a) the beat frequency of $M2$-$S1$, and (b) the injection power ratio of $M2$ to $M1$.

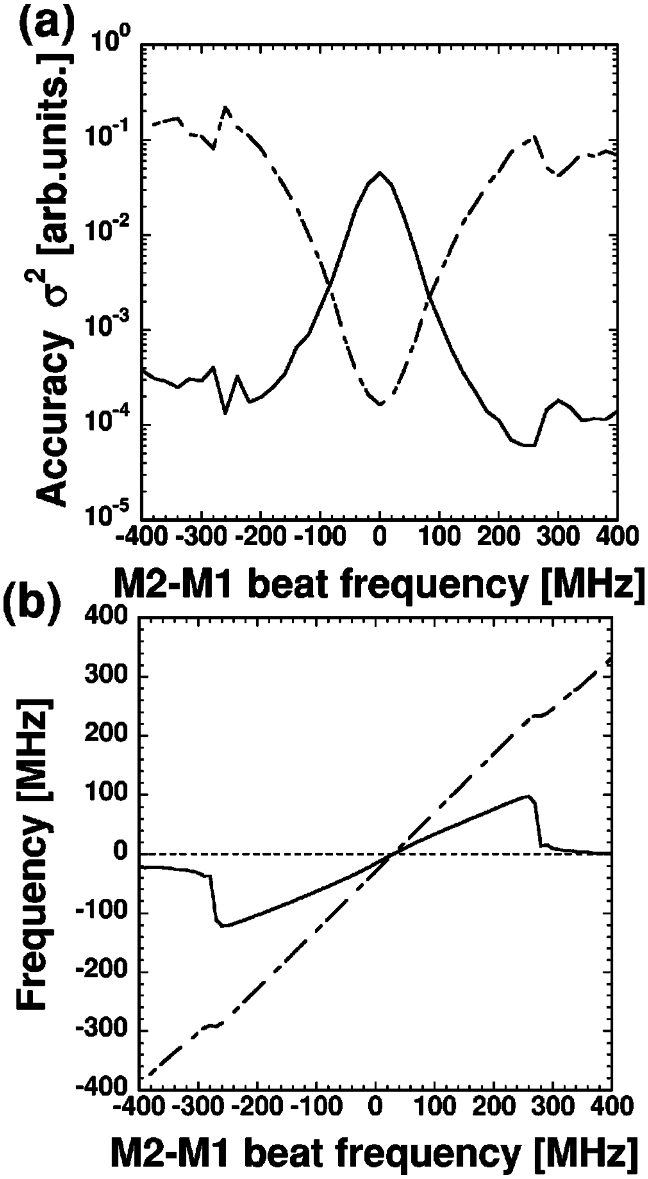

FIG. 8. (a) Numerical results showing accuracy of chaos synchronization for the pair of $M1$-$S1$ (the solid curve) and $M2$-$S1$ (the dashed-dotted curve) as a function of the beat frequency of $M2$-$M1$. (b) Average frequency differences of $S1$ (the solid curve) and $M2$ (the dashed-dotted curve) from $M1$ (the dotted line) as a function of the beat frequency of $M2$-$M1$.

B. Numerical results

During the calculation, we set parameter values of Nd:YVO_4 microchip lasers as follows: lasing wavelength of 1.064 μm, cavity length of 1.0 mm, refractive index of 1.9, and the reflectivities of the cavity mirrors of 99.8% and 99.1% at 1.064 μm. From these values, the photon lifetime in the laser cavity is calculated as $\tau_p = 1.15$ ns. The fluorescent decay time of the upper laser level is set to $\tau = 88$ μs, thus $K = \tau/\tau_p = 7.67 \times 10^4$. When the optical pumping parameter w_0 is set at 1.7, the corresponding relaxation oscillation frequency is 0.42 MHz. To generate chaotic oscillation in a pump modulation system, we set the pump modulation amplitude at $w_p = 0.40$, the pump modulation frequency at $f_p = 0.70$ MHz, and the initial phase of modulation at $\Phi_m = \Phi_s = 0$. All the parameters for the four lasers are set to be identical except the initial conditions.

We calculate the temporal wave forms and correlation plots for the four lasers as shown in Fig. 6. The coupling strengths are set to 50% for all the lasers. In these coupling strengths, the injection-locking range is within 35 MHz. The frequency detunings are set to be small for the corresponding pairs of lasers to achieve injection-locking, i.e., $\Delta\nu_{m1,s1} = \Delta\nu_{m2,s2} = 20$ MHz, whereas they are large enough for different pairs of lasers, i.e., $\Delta\nu_{m1,s2} = \Delta\nu_{m2,s1} = 200$ MHz. Synchronization of chaos is achieved between the corresponding pairs of $M1$-$S1$ and $M2$-$S2$ due to the injection-locking effect. Conversely, synchronization is not achieved for the different pairs of $M1$-$S2$ and $M2$-$S1$. We can achieve dual synchronization of chaos when the frequency detuning is adjusted. These results are consistent with our experimental observations shown in Fig. 2.

We also calculate the influence of injection light in a slave laser from the other pair of the master laser. Figure 7 shows

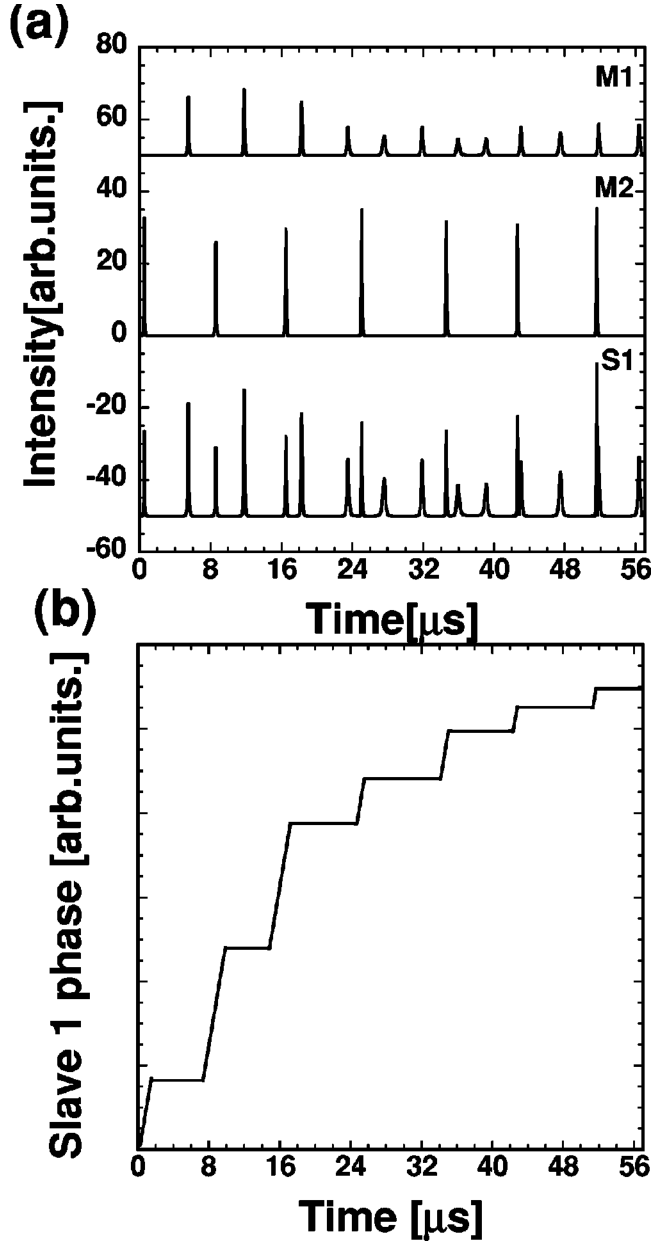

FIG. 9. (a) Temporal wave forms of $M1$, $M2$, and $S1$, and (b) phase dynamics of $S1$ under the small beat frequency of $M2$-$M1$ (150 MHz).

the accuracy of chaos synchronization for $M1$-$S1$ as a function of the beat frequency of $M2$-$S1$ [Fig. 7(a)] and the injection power ratio of $M2$ to $M1$ [Fig. 7(b)]. These numerical calculations in Fig. 7 agree with our experimental results in Fig. 3, where synchronization of chaos for $M1$-$S1$ degrades as the beat frequency of $M2$-$S1$ or the injection power of $M2$ approaches its injection-locking range. Thus we have confirmed numerically that dual synchronization of chaos can be achieved in two pairs of microchip lasers when the optical frequencies are locked only between the corresponding pairs of microchip lasers.

We calculate the accuracy of synchronization not only for $M1$-$S1$ but also for $M2$-$S1$ when the beat frequency of $M2$-$M1$ is changed as shown in Fig. 8(a). As the frequency of $M2$ approaches to the frequencies of $M1$ and $S1$, the accuracy for $M2$-$S1$ is improved, whereas the accuracy of $M1$-$S1$ is degraded. These results correspond to our experimental result shown in Fig. 5. To confirm frequency dynamics of dual synchronization, we calculate the average frequency differences of $S1$ and $M2$ from $M1$ by using Eqs. (3.13) and (3.14), when the frequency of $M2$ is changed as well in Fig. 8(a). Figure 8(b) shows the average frequency differences of $S1$ (the solid curve) and $M2$ (the dashed-dotted curve) from $M1$ (the dotted line). At large frequency of $M2$, the frequency of $S1$ is locked to $M1$, which is a normal injection-locking effect. As the frequency of $M2$ approaches that of $M1$, the frequency of $S1$ is pulled to that of $M2$ and the average frequency of $S1$ moves between $M1$ and $M2$. Therefore, the injection-locking between $M1$ and $S1$ is degraded due to the $M2$ injection.

Figure 9 shows the temporal dynamics of $M1$, $M2$, and $S1$, and the corresponding phase dynamics of $S1$ at the detuning of $M2$-$M1$ of 150 MHz under the injection of the two master lasers. There are stepwise variations for phase dynamics. The values of slopes of the phase dynamics correspond to frequency detuning of $S1$-$M1$, i.e., 0 and 120 MHz, which correspond to the frequency differences of $M1$-$S1$ and $M2$-$S1$. While the pulses of $M1$ are injected into the $S1$ laser, the frequency difference of $M1$-$S1$ is equal to zero, which implies injection-locking is achieved for $M1$-$S1$. On the other hand, the frequency of $M2$ is locked to that of $S1$ only in the presence of the $M2$ pulses. Therefore, the frequency of $S1$ is locked to that of either $M1$ or $M2$, and the locking is automatically switched between $M1$ and $M2$, which depends on the presence of the injected pulses from either of the two master lasers. Therefore, synchronization is instantaneously achieved between $M1$-$S1$ and $M2$-$S1$ during the duration of injection-locking. The injection-locking and synchronization phenomena in one-way coupled multiple pairs of lasers are different from the case for the synchronization in a single pair of lasers.

IV. CONCLUSION

We have experimentally demonstrated the dual synchronization of chaos in two pairs of Nd:YVO_4 microchip lasers in a one-way coupling configuration over one transmission channel. Dual synchronization is achieved when the optical frequency is matched between the corresponding pairs of lasers by using injection-locking. The accuracy of synchronization between $M1$ and $S1$ is degraded as the injection power of $M2$ into $S1$ is increased or the detuning frequency between $M2$ and $S1$ is decreased. The achievement of injection-locking for the corresponding pairs of lasers is important for the dual synchronization. We have confirmed the dual synchronization of chaos by numerical calculation. The frequency of the $S1$ is locked to that of either $M1$ or $M2$ under two optical injection, and the locking is automatically switched between $M1$ and $M2$, which depends on the presence of the injected pulses from either of the two master lasers.

ACKNOWLEDGMENTS

The authors thank P. Davis for helpful discussions. This work was financially supported by the Sumitomo Foundation, the Telecommunications Advancement Foundation, the Sasakawa Scientific Research Grant from the Japan Science Society, the Promotion and Mutual Aid Corporation for Private Schools of Japan, and a Grant-in-Aid for Encouragement of Young Scientists from the Japan Society for the Promotion of Science.

[1] G.D. VanWiggeren and R. Roy, Science **279**, 1198 (1998).

[2] J.-P. Goedgebuer, L. Larger, and H. Porte, Phys. Rev. Lett. **80**, 2249 (1998).

[3] K. Yoshimura, Phys. Rev. E **60**, 1648 (1999).

[4] H.G. Winful and L. Rahman, Phys. Rev. Lett. **65**, 1575 (1990).

[5] J.R. Terry, K.S. Thornburg, Jr., D.J. DeShazer, G.D. VanWiggeren, S. Zhu, P. Ashwin, and R. Roy, Phys. Rev. E **59**, 4036 (1999).

[6] Y. Oishi and K. Nemoto, Jpn. J. Appl. Phys., Part 2 **39**, L975 (2000).

[7] L.S. Tsimring and M.M. Sushchik, Phys. Lett. A **213**, 155 (1996).

[8] Y. Liu and P. Davis, Phys. Rev. E **61**, R2176 (2000).

[9] A. Uchida, T. Ogawa, M. Shinozuka, and F. Kannari, Phys. Rev. E **62**, 1960 (2000).

[10] A.E. Siegman, *Lasers* (University Science Book, Mill Valley, CA, 1986).

[11] C.L. Tang, H. Statz, and G. deMars, J. Appl. Phys. **34**, 2289 (1963).